The Journal of Neuroscience, December 15, 1997, 17(24):9393–9406

Differential Dependence on GluR2 Expression of Three Characteristic Features of AMPA Receptors

Mark S. Washburn, Markus Numberger, Sunan Zhang, and Raymond Dingledine

Department of Pharmacology, Emory University School of Medicine, Atlanta, Georgia 30322

The GluR2 subunit controls three key features of ion flux through the AMPA subtype of glutamate receptors—calcium permeability, inward rectification, and channel block by external polyamines, but whether each of these features is equally sensitive to GluR2 abundance is unknown. The relations among these properties were compared in native AMPA receptors expressed by acutely isolated hippocampal interneurons and in recombinant receptors expressed by *Xenopus* oocytes. The shape of current–voltage (*I–V*) relations between −100 and +50 mV for either recombinant or native AMPA receptors was well described by a Woodhull block model in which the affinity for internal polyamine varied over a 1000-fold range in different cells. In oocytes injected with mixtures of GluR2:non-GluR2 mRNA, the relative abundance of GluR2 required to reduce the log of internal blocker affinity by 50% was two- to fourfold higher than that needed to half-maximally reduce divalent permeability or channel block by external polyamines. Likewise, in interneurons the affinity of externally applied argiotoxin for its blocking site was a steep function of internal blocker affinity. These results indicate that the number of GluR2 subunits in AMPA receptors is variable in both oocytes and interneurons. More GluR2 subunits in an AMPA receptor are required to maximally reduce internal blocker affinity than to abolish calcium permeability or external polyamine channel block. Accordingly, single-cell RT-PCR showed that approximately one-half of the physiologically characterized interneurons exhibiting inwardly rectifying AMPA receptors expressed detectable levels of edited GluR2. The physiological effects of a moderate change in GluR2 relative abundance, such as occurs after ischemia or seizures or after chronic exposure to morphine, thus will be dependent on the ambient GluR2 level in a cell-specific manner.

Key words: AMPA receptor; glutamate receptor; spider toxin; hippocampal interneuron; GluR2 subunit; RT-PCR; kainate; patch clamp; stratum radiatum; inward rectification; polyamine; spermine; calcium permeability; CA3; argiotoxin; Woodhull

The subunit stoichiometry of muscle nicotinic acetylcholine receptors is fixed ($\alpha_2\beta\gamma\delta$ or $\alpha_2\beta\gamma\epsilon$) because of a prescribed order of subunit assembly in which preformed $\alpha\delta$ and $\alpha\gamma$ dimers subsequently are bridged by a β subunit (Gu et al., 1991). Fixed subunit stoichiometry limits the scope of functional diversity in muscle endplate receptors. Current evidence indicates that other ligand-gated ion channels also exhibit fixed or strongly preferred subunit stoichiometry rather than a stoichiometry determined by random assembly of subunits [Cooper et al. (1991) for neuronal nicotinic, Kellenberger et al. (1997) and Tretter et al. (1997) for $GABA_A$, and Kuhse et al. (1993) for glycine receptors], but this issue has not been examined for glutamate receptors, which mediate the vast majority of fast excitatory transmission in the brain. The AMPA subtypes of glutamate receptors are assembled from the GluR1–4 subunits and exhibit a wide range of functional diversity that is dependent on which subunits are present. Several important features of ion permeation through recombinant AMPA receptors depend strongly on the edited GluR2 subunit, including calcium permeability and rectification (Hollmann et al., 1991), sensitivity to channel block by external polyamines (Brackley et al., 1993; Herlitze et al., 1993), and single channel conductance (Swanson et al., 1997).

The ratio of GluR2 to non-GluR2 mRNA levels changes by up to 60% in several pathophysiological conditions, including ischemia and status epilepticus (Pellegrini-Giampietro et al., 1992a; Pollard et al., 1993; Prince et al., 1995), after chronic treatment with morphine or cocaine (Fitzgerald et al., 1996), and during development (Pellegrini-Giampietro et al., 1992b). For this reason it is important to determine whether AMPA receptor properties vary with *moderate* changes in GluR2 level.

A key question in bridging the information provided by molecular biological and electrophysiological approaches is whether functional properties of recombinant subunit combinations faithfully predict those of native AMPA receptors. The likelihood of cell-specific differences in post-translational processing or receptor assembly makes it important to examine this issue for each case. One approach is the study of mice deficient in GluR2 editing (Brusa et al., 1995) or lacking the GluR2 gene (Jia et al., 1996). The calcium permeability of AMPA receptors in neurons from these mice is expectedly high in the absence of edited GluR2, but little additional information is available. A second approach is functional phenotyping and genetic analysis in the same neuron (Lambolez et al., 1992; Mackler and Eberwine, 1993; Bochet et al., 1994; Geiger et al., 1995; Ruano et al., 1995). Using this method, Bochet et al. (1994) concluded that cultured hippocampal neurons exhibiting inwardly rectifying AMPA receptors never

Received June 3, 1997; revised Sept. 22, 1997; accepted Sept. 24, 1997.

This work was supported by a National Research Service Award Fellowship (to M.S.W.), a Boehringer–Ingelheim Fellowship and the Markey Foundation (to M.N.), a National Institutes of Health grant (to R.D.), and the Bristol-Myers Squibb Company. We thank Steve Traynelis for insightful comments on an early draft of this manuscript, Jeanne Peters for sequencing PCR fragments amplified from interneurons, and Roger Dingledine for programming assistance.

Correspondence should be addressed to Dr. Raymond Dingledine, Department of Pharmacology, Emory University School of Medicine, Atlanta, GA 30322.

Dr. Washburn's present address: SIBIA Neurosciences Incorporated, 505 Coast Boulevard South, Suite 300, La Jolla, CA 92037.

Dr. Numberger's's present address: Department of Neurophysiology, Humboldt University, Tucholskystrasse 2, 10017 Berlin, Germany.

 0270-6474/97/179393-14$05.00/0

express the GluR2 or GluR3 subunits. Single-cell RT-PCR results from neurons of numerous brain regions suggest that a single GluR2 subunit in native AMPA receptors may be sufficient to maximally reduce calcium permeability (Geiger et al., 1995). However, it is not known whether all of the phenotypic consequences of GluR2 expression are equally sensitive to GluR2. Our work addresses this issue in oocytes expressing recombinant AMPA receptors and in hippocampal interneurons isolated from CA3 stratum radiatum (McBain and Dingledine, 1993). Our results provide strong evidence that the number of GluR2 subunits in AMPA receptors is variable, which could contribute to extensive physiological diversity at glutamatergic synapses.

MATERIALS AND METHODS

Interneuron recordings. To acutely dissociate interneurons, we prepared hippocampal slices (400 μm) from male Sprague Dawley rat pups (10–16 d postnatal). Slices were cut with a Vibratome in cold oxygenated artificial CSF (ACSF) consisting of (in mM) 124 NaCl, 3.5 KCl, 1.3 $MgCl_2$, 26.0 $NaHCO_3$, 10 glucose, and 2.0 $CaCl_2$. Slices were digested enzymatically at 32°C for 12 min in normal ACSF with Pronase E (1.5 mg/ml, Sigma, St. Louis, MO). This solution typically contained elevated Mg^{2+} (5 mM), reduced Ca^{2+} (0.8 mM), and the nonselective glutamate receptor antagonist kynurenic acid (1 mM) to minimize glutamate receptor-induced excitotoxicity. After digestion, slices were washed five times with normal ACSF and stored in continuously oxygenated ACSF at room temperature until trituration. Then the stratum radiatum–stratum lacunosum/moleculare region of CA3 was microdissected from three to five slices and minced into smaller pieces (~0.25 mm^2). Tissue pieces were triturated in HEPES-buffered DMEM, pH 7.35–7.4 (320 mOsm; Life Technologies, Gaithersburg, MD) containing trypsin inhibitor (0.68 mg/ml; Sigma) by repeatedly passing them through a series of glass fire-polished Pasteur pipettes with decreasing tip diameters. Cells were plated onto plastic coverslips coated with CellTak (Collaborative Biomedical, Bedford, MA). Acutely dissociated cells exhibited several morphologies. The majority (82%) of small oval cells accumulated [^{3}H]GABA in a sodium-dependent manner (data not shown). These neurons were presumably GABAergic because GAD expression is correlated with [^{3}H]GABA uptake in culture (Hoch and Dingledine, 1986). Approximately one-half of the small multipolar cells accumulated [^{3}H]GABA, whereas only 4% of the pyramidal-shaped cells did so. These data are consistent with the idea that the majority of neurons isolated from the strata radiatum and lacunosum moleculare are GABAergic. Electrophysiological recordings were restricted to the small oval or multipolar cells.

Conventional whole-cell voltage-clamp recordings were obtained from interneurons by using glass microelectrodes filled with internal solution consisting of (in mM) 140 cesium methanesulphonate, 10 HEPES, and 2 $MgCl_2$ (280 mOsm, adjusted to pH 7.25–7.3 with CsOH). Electrode glass was baked (200°C for >2 hr) before use. Electrodes were filled with 8 μl of internal solution that had been prepared with DEPC-treated water and had been UV-treated before use. Tip resistances were 4–6 MΩ. External recording solution contained (in mM) 142 NaCl, 1.5 KCl, 10 HEPES, 10 glucose, 20 sucrose, 2.0 $CaCl_2$, and 1.3 $MgCl_2$, pH 7.35–7.4 (315–320 mOsm). Recordings were amplified (Axoclamp 200, Axon Instruments, Foster City, CA) and displayed on an oscilloscope and chart recorder. Signals also were fed to a computer interface (TL-1, Axon Instruments), which digitized the analog waveforms for analysis by microcomputer-based programs (pClamp or Axograph from Axon Instruments, and Origin for Windows from Microcal Software, Northampton, MA). Ramp *I–V* relations were generated by holding the membrane potential at +50 mV and ramping to −100 mV over a 2 sec period. The use of this protocol resulted in the inactivation of many voltage-dependent conductances and therefore less complicated *I–V* relations. Leak current at −100 mV was typically <10% of the kainate-evoked current. Kainate *I–V* relations were calculated by subtracting the average of the leak currents obtained before and after 300 μM kainate application from that obtained in the presence of agonist. After recording, the entire cell was aspirated into the recording electrode for subsequent molecular analysis.

Data analysis. For comparison with previous studies, the kainate rectification ratio was calculated by dividing the slope of the kainate-induced *I–V* relation measured between +35 and +45 mV by the slope between −65 and −75 mV. For determination of P_{Ca}/P_{Na}, the reversal potential of kainate-evoked currents was measured in both high sodium and high calcium solutions, and the analysis described by Geiger et al. (1995) followed. High sodium solution consisted of (in mM) 135 NaCl, 5.4 KCl, 1.8 $CaCl_2$, 1.0 $MgCl_2$, and 5 HEPES, pH 7.2 with NaOH. High calcium solution consisted of 100 mM $CaCl_2$ plus 5 mM HEPES, pH 7.4. To facilitate rapid solution exchange, we lifted cells from the bottom of the dish into a stream of perfusion solution, which was focally applied to the cell under study via 200 μm quartz tubing. Then:

$$P_{Ca}/P_{Na} = 0.25 \cdot (a_{Na}/a_{Ca}) \cdot \exp[(2 \cdot E_{Ca} - E_{Na})/25.3] + \exp[(E_{Ca} - E_{Na})/25.3], \quad (1)$$

where a_{Na} = Na^+ activity (activity coefficient = 0.75), a_{Ca} = Ca^{2+} activity (activity coefficient = 0.55), E_{Ca} = reversal potential of kainate-evoked current measured in high calcium solution, and E_{Na} = reversal potential measured in high sodium solution. This equation assumes negligible interaction between permeating ions and assumes negligible surface charge effects. E_{Ca} was adjusted for an estimated junction potential of +10 mV when locally applied solution was changed from high sodium to high calcium.

AMPA receptor *I–V* curves were described by a Woodhull model of internal channel block by impermeable blocker ions, which is appropriate for AMPA receptor channels between −100 and +50 mV (Bowie and Mayer, 1995). The current (I_v) at each membrane voltage (V) was fit by a least-squares criterion to the following equation:

$$I_v = G_v(V - V_{rev}), \quad (2)$$

where V_{rev} is the reversal potential and G_v is the voltage-dependent channel conductance. To a first approximation, the block can be modelled as a simple bimolecular interaction of nonpermeant internal blocking ions with their binding site in the channel:

$$G_v = G_o[1/(1 + \text{blocker}/K_{D_v})]. \quad (3)$$

The affinity of internal blocking ions for their binding site (K_{D_v}) is a function of voltage according to the Woodhull equation:

$$K_{D_v} = Kd(0)\exp[-z(1 - \delta)VF/RT], \quad (4)$$

where $K_D(0)$ is the blocker dissociation constant at 0 mV, z is the effective valence of the cytoplasmic blocker, δ is the electrical distance through the membrane of the blocking site (measured from the extracellular side of the channel), and RT/F = 25.3 mV at 20°C. The calculated $K_D(0)$ describes the combined action of at least two internal blocking ions (spermine and spermidine). Moreover, the calculated value of $K_D(0)$ depends on the intracellular polyamine concentrations. Although it is highly unlikely that internal polyamine concentration varies systematically depending on GluR2 expression, we use the ratio of $K_D(0)$/[polyamine] as the Woodhull affinity parameter to make possible comparisons between interneurons and oocytes. The cytoplasmic free polyamine concentration has been estimated at 65 μM for hippocampal neurons (Bowie and Mayer, 1995) and at 300 μM for stage V oocytes (Osborne et al., 1989). G_0 in Equation 3 is the channel conductance at each voltage in the absence of internal block and was adjusted by the following equation to produce a rectification ratio of 2.9 to approximate the most outwardly rectifying currents observed in both native (see Fig. 3*C*) and recombinant (see Fig. 1*C*) AMPA receptors:

$$G_0 = 0.3 + 0.6\exp[(V - 50)/40]. \quad (5)$$

It was not necessary to include an extra term corresponding to some fraction of the AMPA receptors that are completely insensitive to the internal blocker, although our analysis does not preclude a mixture of AMPA receptors that are insensitive and variably sensitive to internal polyamines. For example, at low GluR2 expression a mosaic of GluR2-containing and GluR2-lacking receptors is expected. The Woodhull parameters then would reflect a weighted average of a mosaic of receptors that contain 0, 1, 2, etc. GluR2 subunits, if subunit composition is not fixed. Equations 2–5 were incorporated into a program written in LabWindows CVI (National Instruments, Austin, TX). The fitting module used a simplex algorithm provided by Steve Traynelis and Roger Dingledine. *I–V* relations were normalized to the current at −100 mV.

For channel block by external polyamine toxins, the above analysis was performed in the absence of external blocker to derive the parameters for internal block—V_{rev}, $K_D(0)$/[polyamine], and $z(1 - \delta)$—which then were fixed for a second round of fitting in the presence of external blocking ion to the Woodhull equation for external block:

$$Kd_v = Kd(0)\exp[z\delta VF/RT]. \quad (6)$$

Eleven of the 18 neurons were well fit by Equation 6, and $z\delta$ in this population was 1.22 ± 0.06, but the program had difficulty converging for cells with very weak external block (i.e., when the unblocked and blocked *I–V* curves were similar). For this reason the $z\delta$ term was set at 1.22 for all external block fits.

Single-cell RT-PCR. To amplify specific AMPA receptor subunits from single dissociated neurons, we used two different methods, each a variant of the protocol described by Lambolez et al. (1992). For one set of neurons (n = 132) the entire cell was drawn up into the patch pipette after whole-cell recording. Then the pipette tip containing the cell was crushed into a silanized, RNase-free, 0.6 ml tube (Costar, Cambridge, MA) containing 12 μl of reverse transcriptase (RT) solution, and the contents were expelled together with ~8 μl of pipette solution. The composition of the RT solution was (final concentrations) 10 pg/ml random hexanucleotides [Bethesda Research Laboratories, (BRL), Bethesda, MD], and (in mM) 50 Tris-HCl, pH 8.3, 8 $MgCl_2$, 30 KCl, 10 dithiothreitol, and 0.5 dNTP (Pharmacia, Piscataway, NJ). Next, 20 U RNasin (United States Biochemicals, Cleveland, OH) was added immediately, and reverse transcription of cellular RNAs was initiated by the addition of 200 U MMLV-RT (BRL) in a total volume of 21 μl. After incubation at 42°C for 2 hr, the RT reaction was frozen at −20°C until needed for the PCR reaction later that day. We found that the following conditions resulted in higher ^{32}P-dCTP incorporation into reverse-transcribed cRNA: an incubation temperature of 42°C, rather than 37°C; 2 hr, rather than 1 hr of incubation; 8 mM Mg^{2+}, rather than 2 mM; and MMLV RT, rather than AMV or Superscript. To the RT reaction, 30 μl of PCR solution was added containing a pair of pan primers (2 μM each final concentration) specific for GluR1, 2, 3, and 4 (forward primer TGGCCTATGAGATCTGGATGTG; reverse primer CCATAGCCTTTGGA(G/A)TC) and (in mM) 0.2 dNTP, 20 Tris-HCl, pH 8.2, 10 KCl, 6 $(NH_4)_2SO_4$, and 5 $MgCl_2$ with 0.1% Triton X-100, 10 μg/ml BSA, and 2.5 U Pfu-polymerase (Stratagene, La Jolla, CA). Hot-start PCR was performed in a Thermal Cycler 480 (Perkin-Elmer, Norwalk, CT) for 40 cycles at 94, 45, and 72°C for 30, 45, and 80 sec. Pfu polymerase was found to be more reliable than Pfu-exo$^-$. PCR products were isolated by anion exchange chromatography [Wizard PCR cleaning columns from Promega (Madison, WI), which gave higher recovery than Bio-Rad or Clontech 100 columns], and ~10% of the PCR reaction was used for a second PCR run in which each GluR subunit was amplified separately with the following nested primers: GluR1 forward, GTCGTCCTCTTCCTGGTCAGCC, and reverse, GTGTCACAGGGCTTTCGTTGCT; GluR2 forward, TCAGCAGATTTAGCCCCTACGA, and reverse, GCATACTTTCCTTTGGATTTCC; GluR3 forward, TAGTCAGCAGATTTAGCCCTTA, and reverse, TTTCCACCAACTTTCATCGTAT; GluR4 forward, ATCGTCCTACACTGCTAATCT, and reverse, ACGATGAAAGTGGGAGGAAACC.

The second reaction was initiated by hot start and then cycled 40 times at 94, 55, and 72°C for 30, 45, and 80 sec in a total volume of 50 μl [reaction conditions (in mM): 0.2 dNTP, 20 Tris-HCl, pH 8.2, 10 KCl, 6 $(NH_4)_2SO_4$, and 2 $MgCl_2$ with 0.1% Triton X-100, 10 μg/ml BSA, 2 μM each primer, and 2.5 U Pfu-polymerase]. The presence or absence of PCR bands indicative of GluR1–GluR4 mRNAs was determined by running 30% of the second PCR sample on a 1.2% agarose gel and visualizing the ethidium-stained PCR fragments under UV light. The expected sizes of the PCR bands were 541, 475, 558, and 341 bp for GluR1–GluR4, respectively. Restriction digests were used in early experiments to verify the identify of the PCR bands as described by Lambolez et al. (1992). In 11 cells, PCR bands were subcloned and sequenced to confirm identification of the PCR products. In all cases the restriction patterns were appropriate, and the sequence confirmed the identity of the PCR bands. The primer pairs were selected to span one or more introns of the AMPA receptor genes, so we can be confident that the PCR bands shown do not represent amplification of genomic DNA or unspliced RNA.

In an attempt to improve on the success rate obtained by using the protocol described above, for a second group of neurons (n = 150) we used parts of the Lysate mRNA Capture Kit (United States Biochemicals) to prebind the poly(A^+) RNA to a poly-dT membrane. A neuron was expelled together with the pipette solution into a silanized, RNase-free 0.6 ml tube (Costar) containing 10 μl of lysis solution (4 M guanidinium thiocyanate, 25 mM Na-citrate, and 0.5% *N*-lauroylsarcosine). Immediately, 20 μl of ENN (500 mM NaCl and 1% Nonidet-P 40) and one poly-dT membrane were added. After 1 hr of slow shaking at room temperature, the solution was removed and the membrane washed twice with 200 μl of 50 mM KCl and 10 mM Tris, pH 8.3. After binding the mRNA to the membrane, we performed the RT reaction as well as the first PCR run in the same tube containing this membrane, as described above.

Because of the extreme sensitivity of 40 cycle PCR, precautions were taken to minimize contamination of the solutions with cellular RNA or plasmid DNA present in the laboratory. First, all solutions and the glass micropipettes were exposed to UV light to degrade long DNA and RNA templates. Second, the RT reactions and PCR setup were done in a room not used for manipulations involving plasmids. Third, aerosol-resistant pipette tips were used routinely. Fourth, all solutions were tested by RT-PCR for the absence of contaminating AMPA receptor RNA or DNA, distributed into single-experiment aliquots, and stored at −20°C until shortly before use. Finally, one or more control experiments were performed in each recording session by placing the tip of an electrode near the bottom of the recording chamber and aspirating the recording solution. Then a molecular analysis for GluR1–4 subunits was performed on the aspirated solution in parallel with that performed on harvested neurons. In a typical experiment five neurons plus the control pipette solution were processed together. Results from all neurons were discarded if any AMPA receptor PCR products were amplified from the negative control.

Methodological considerations for single-cell RT-PCR. PCR bands indicative of AMPA receptor subunits were recovered from ~30% of the cells harvested. We considered several possible sources for the low yield, including sensitivity of the assay, adsorption of cellular RNA by the glass patch pipette, and the method for harvesting cellular RNA. First, neither neuron soma area measured from scanned photographs of individual neurons with National Institutes of Health Image software, which varied from 120 to 750 μm^2, nor kainate response amplitude, which varied between 200 and 2200 pA at −60 mV, was a good predictor of the ability to recover PCR bands from individual neurons (n = 95 neurons; data not shown). This suggests that neither the amount of cytoplasm harvested nor the density of functional AMPA receptors expressed by a neuron was a major determinant of the success rate of RT-PCR.

Second, we tested whether adsorption of RNA by the different types of glass patch pipettes reduced the amount of RNA available to the RT reaction. Glass pipette blanks were loaded for 15 min with 8 μl of internal recording solution containing ^{32}P-GluR3 cRNA at a concentration of 25 pg/ml and then rinsed quickly three times with distilled water; the radioactivity associated with both glass and solution was determined separately by liquid scintillation counting. Lead phosphate glass (Corning 8161, supplied by World Precision Instruments, Sarasota, FL) absorbed 33 ± 1% of the RNA, whereas the harder N51A borosilicate glass (Drummond, Broomall, PA) bound only 2.0 ± 0.5% of the RNA (n = 5 or 6 pipettes each). Binding of RNA to the Corning 8161 glass was reduced to 5.0 ± 0.4% (n = 4) by presoaking the glass with internal solution containing 5 μM dNTP. Although this experiment indicates that RNA preferentially adheres to "soft" glass, switching from soft to hard pipette glass did not improve the success rate, further suggesting that the ability to recover RNA from cells was not limiting.

Finally, because the entire cell was harvested for the RT reaction, we considered the possibility that a cellular component interferes with reverse transcription of mRNA. This was tested by absorbing the RNA to a poly-dT membrane and rinsing the membrane thoroughly before the RT reaction. The PCR bands resulting from reverse transcription and amplification of 10 fg or 1 pg of GluR2 cRNA were the same intensity in direct comparisons of both methods, indicating that binding of mRNA by the poly-dT membrane is efficient. Indeed, of 132 interneurons harvested with the original method (Lambolez et al., 1992), RT-PCR was successful with 30 cells (23%); by contrast, RT-PCR bands were recovered successfully in 61 of 150 cells (41%) harvested with the poly-dT membrane. The observed pattern of AMPA receptor expression by interneurons was similar with both methods, so we tentatively conclude that adsorption of mRNA to poly-dT membranes may be more effective for recovering small amounts of mRNA from individual cells.

These results, taken together, are consistent with the caveat that the copy number of AMPA receptor subunit mRNA molecules per cell approaches the detection threshold with this assay. This conclusion may

seem to conflict with other reports of single-cell RT-PCR used to quantitate mRNA levels, but previous studies either amplified 1000-fold higher concentrations of cRNA than are expected to be present in a single neuron (Lambolez et al., 1992), or femtogram levels of *cDNA* rather than cRNA (Geiger et al., 1995). To our knowledge it has not yet been possible to convincingly quantify the relative levels of low-abundance mRNAs found in individual neurons by an RT-PCR approach. For these reasons the absence of a PCR band is difficult to interpret in a particular cell, although one can be confident that the presence of a PCR band (e.g., for GluR2 in some type 2 neurons) is indicative of the presence of the mRNA.

Expression of AMPA receptors in oocytes. The procedure for preparation and injection of *Xenopus* oocytes followed that of Dingledine et al. (1992). Briefly, stage V–VI oocytes were isolated from anesthetized frogs, enzymatically treated by gentle shaking with collagenase (Type IV, 1.3 mg/ml for 45–70 min; Worthington, Freehold, NJ) in a calcium-free Barth's solution, and then manually defolliculated. Cells were injected with 5–60 ng of mRNA transcribed from linearized constructs in the pBluescript vector (Stratagene). For coexpression of GluR2 with other subunits, GluR2 mRNA was injected at different ratios to GluR3 or equimolar mixtures of GluR1 plus GluR3 or GluR3 plus GluR4; total RNA injected was held to 60 ng or less. Injected oocytes were maintained at 17°C in Barth's solution containing penicillin and streptomycin (50 μg/ml) for 2–10 d, after which two-electrode voltage-clamp recordings were made at room temperature from cells continually perfused in a standard frog Ringer's solution. This solution was composed of (in mM) 88 NaCl, 1.0 KCl, 24 $NaHCO_3$, 10 HEPES, 0.4 $MgCl_2$, and 0.1 $CaCl_2$. Recording pipettes were filled with 3 M CsCl and 0.4 M EGTA, pH 7.5, to chelate Ca^{2+} and thereby minimize the activation of calcium-dependent chloride currents. Kainate-induced currents typically were elicited from a holding potential of −70 mV. Kainate (30–300 μM) was used as an agonist for AMPA receptors because it desensitizes much less than does glutamate or AMPA itself. Current–voltage (*I–V*) relationships were generated by applying a 2 sec ramp depolarization from −70 or −100 mV to +50 mV. In these experiments the average of the leak current obtained by applying the voltage ramp before and after kainate application was subtracted from the current obtained in the presence of agonist.

$P_{Ba}/P_{monovalent}$ was estimated from reversal potential measurements in high Na solution (in mM): 90 NaCl, 1 KCl, 1.8 $MgCl_2$, 0.1 $CaCl_2$, and 15 HEPES, pH to 7.5 with ~7.5 mM NaOH, and in high Ba solution (in mM): 60 $BaCl_2$, 1.8 $MgCl_2$, and 15 HEPES, pH to 7.5 with ~3.5 $Ba(OH)_2$. Equation 1 was used, but E_{Ba} was corrected for a +10 to +11 mV junction potential. Care was taken to measure E_{Ba} shortly after the onset of the kainate-activated current, and the kainate concentration was typically kept low (30 μM) to reduce calcium influx and thereby further minimize contamination by calcium-dependent chloride currents. Under these conditions two successive ramps usually yielded *I–V* relations that reversed within 1 mV of each other.

RESULTS

Graded inward rectification in recombinant AMPA receptors

The shape of the *I–V* curve for native AMPA receptors expressed by CA3 stratum radiatum interneurons or for oocytes injected with AMPA receptor mRNAs in various ratios varies from strong inward rectification to moderate outward rectification. The ratio of slope conductances measured at +40 and −70 mV ranges from 0.005 to ~3. Such a wide range of rectification properties is unlikely to be attributable solely to variation in cytoplasmic polyamine concentration among oocytes or CA3 interneurons, because Ca^{2+} permeability and channel block by external polyamines also varied over at least two orders of magnitude (see below). To gain insight regarding other mechanisms that might give rise to *I–V* curves with varying degrees of rectification in different neurons, we first studied AMPA receptors formed by oocytes injected with mRNAs encoding GluR2 and non-GluR2 subunits in different ratios. The solid lines in Figure 1*A* show three *I–V* curves representing the extremes of inward (1:0:1 GluR1:R2:R3 mRNA injection ratio) and outward (1:10:1) rectification plus an intermediate case (the 5:2:5 injection ratio). Each curve is the average of from three to five oocytes, all obtained from the same frog. Because a fixed or highly preferred subunit stoichiometry is thought to occur in neuronal nicotinic (Cooper et al., 1991), $GABA_A$ (Kellenberger et al., 1997; Tretter et al., 1997), and glycine (Kuhse et al., 1993) receptors, we first considered whether the intermediate *I–V* curve could result solely from a mixture of two AMPA receptor subtypes, those containing or lacking the GluR2 subunit. If the number of GluR2 subunits in a receptor were fixed, as is the case for α subunits of muscle nicotinic receptors (termed the "fixed stoichiometry" model for simplicity), the macroscopic *I–V* curve would be built up from the sum of *I–V* curves from all individual receptors, each of which has one or the other extreme shape. This model predicts that all intermediate *I–V* curves would be weighted averages of the two extreme *I–V* curves. Accordingly, an attempt was made to fit the intermediate *I–V* curve at each voltage to the following equation: $I_{5:2:5} = A \cdot I_{1:0:1} + (1 - A) \cdot I_{1:10:1}$, where A is the fraction of receptors assembled in the absence of GluR2. However, the open circles in Figure 1*A*, which represent the hypothetical case of 52% outwardly rectifying channels and 48% inwardly rectifying channels, fit the negative limb of the 5:2:5 *I–V* curve but diverge markedly from the positive limb. These weighting factors were chosen to approximate the inward limb of the *I–V* curve, but weighting factors chosen to fit the outward limb do not accurately describe the inward limb of the intermediate *I–V* curve, because the resulting *I–V* curve lies much closer to the inwardly rectifying (1:0:1) curve than to the 5:2:5 curve (data not shown). Similar experiments performed with oocytes injected with GluR2/R3, GluR3/R3(R612), or GluR2/R3/R4 mRNAs or with native AMPA receptors (e.g., Fig. 3*A*) indicate that the fixed stoichiometry model does not describe the data accurately.

The rectification ratio and the shape of a plot of this ratio versus GluR2 abundance are markedly influenced by the voltages chosen to measure conductance, making the rectification ratio itself generally unsuitable to describe the degree of rectification. Inward rectification of AMPA and kainate receptors is caused by voltage-dependent channel block by internal polyamines (Bowie and Mayer, 1995; Donevan and Rogawski, 1995; Kamboj et al., 1995; Koh et al., 1995). The Woodhull model of channel block by nonpermeant internal polyamines has been shown to provide an adequate fit to fully inwardly rectifying *I–V* curves of AMPA receptors lacking GluR2 for voltages more negative than +50 mV (Bowie and Mayer, 1995). Figure 1*A* (*solid circles*) shows that the Woodhull model also provides a satisfactory fit to both inward and outward limbs of the intermediate *I–V* curve, *provided* that the affinity of the cytoplasmic blocking ion for its binding site in the channel, $K_D(0)$, is allowed to vary. The adequacy of the Woodhull model with variable blocker affinity is shown further by a more extended series of GluR1/R2/R3 injection ratios in Figure 1*B*, for GluR2/R3 receptors in Figure 1*D*, and for interneurons discussed below. From inspection of these families of *I–V* curves it is clear that the fixed stoichiometry model is inappropriate, because in each case the inward limb is more sensitive to low GluR2 levels than is the outward limb. If the sole effect of increasing GluR2 abundance were to increase the proportion of receptors that contained a fixed number of GluR2 subunits, then a given shift in the inward limb would be mirrored by a proportionate shift in the outward limb. This

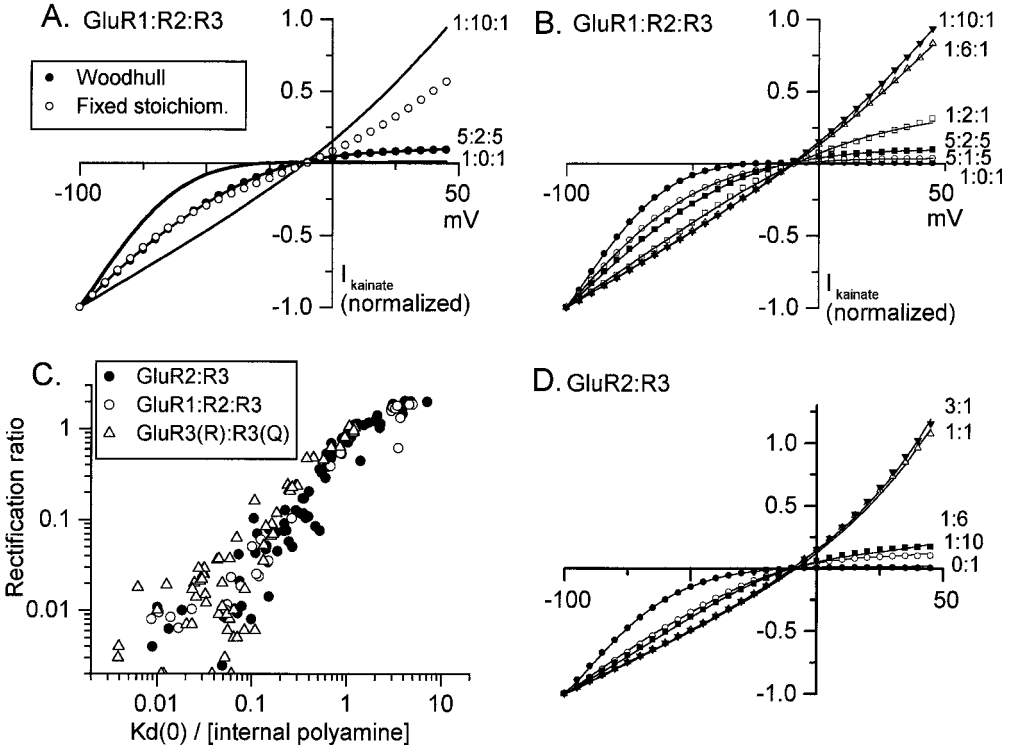

Figure 1. Comparison of the fixed stoichiometry and Woodhull models for intermediate *I–V* curves. *A*, *I–V* curves of kainate-evoked currents in oocytes injected with mixtures of GluR1, 2, and 3 mRNAs in the ratios indicated to the *right* of each *I–V*. The *open circles* represent a weighted average of the 1:0:1 and 1:10:1 curves, with weighting factors chosen to fit the inward limb of the intermediate (5:2:5) *I–V* curve. The *filled circles* represent the Woodhull model fit of the 5:2:5 curve [$K_D(0)$/[polyamine] = 0.35, $z(1 - \delta) = 0.85$]. Each *I–V* curve is the normalized average from three to five oocytes. *B*, Effect of varying the relative abundance of GluR2 on the shape of kainate *I–V* relations in oocytes injected with mRNA encoding GluR1:R2:R3. Each of the *I–V* relations was generated from oocytes obtained from a single frog, and the Woodhull fits (*symbols*) are superimposed. Note that the inward limb of the 1:10:1 and 1:6:1 *I–V* curves are superimposed. Each curve is the normalized average of three to five oocytes. *C*, Relation between the rectification ratio (slope conductance ratio measured at +40 and −70 mV) and apparent affinity of cytoplasmic polyamine blocker for the channel ($n = 116$ oocytes injected with mixtures of the mRNA combinations indicated). GluR2:R3 mRNAs were injected in the following ratios: 0:1, 1:10, 1:3, 1:1, 3:1, 6:1, and 10:1. GluR1:R2:R3 were injected in ratios of 1:0:1, 5:1:5, 5:2:5, 5:3.33:5, 1:2:1, 1:6:1, and 1:10:1. *D*, A family of *I–V* curves in oocytes injected with the indicated ratios of GluR2:GluR3 mRNAs. Each curve is the normalized average from several oocytes ($n = 76$ total), and the Woodhull fits (*symbols*) are superimposed. Inspection of the inward and outward limbs of the *I–V* curves shows that the degree of rectification of the 1:6 and 1:10 *I–V* curves cannot be described by the fixed stoichiometry model. Note that the inward limbs of the 3:1 and 1:1 *I–V* curves are superimposed.

was not observed. For example, in Figure 1*D* the inward limb of the $R2:R3_{1:10}$ curve is shifted halfway between the two extremes, but the outward limb is very close to that of fully rectifying GluR3 receptors, presumably because of the voltage dependence of channel block that underlies inward rectification.

GluR2 abundance did not influence the reversal potential in solutions containing high monovalent and low divalent ion concentrations (Fig. 1*B,D*), which indicates that, in contrast to GluR6 kainate receptors (Burnashev et al., 1996), GluR2 has little or no influence on monovalent ion selectivity in AMPA receptors. However, the gradual reduction of internal blocker affinity as the relative GluR2 abundance is increased implies that the structure of the binding site for the blocking ion is different for AMPA receptors assembled with increasing numbers of GluR2 subunits. Indeed, Figure 1*C* shows that, in a series of oocytes injected with different mRNA mixtures, both internal blocker affinity and the rectification ratio varied over nearly three orders of magnitude. Similar results were obtained with mixtures of GluR3(R612) and GluR3(Q612) mRNAs (Fig. 1*C*), indicating that the *number* of arginine residues in the Q/R site position is the relevant determinant of the degree of rectification of AMPA receptor *I–V* curves.

Multiple subunit stoichiometries in recombinant AMPA receptors

The results presented above suggest that AMPA receptors contain a variable number of GluR2 subunits and that the number of GluR2 subunits in a receptor influences the degree of rectification. To examine this hypothesis in more detail, we compared, in the same oocyte, the GluR2 dependence of three features of permeation through recombinant AMPA receptors. *Xenopus* oocytes prepared from a single frog were injected with mixtures of GluR2 and GluR3 mRNAs or GluR1/R2/R3 or GluR2/R3/R4 mRNAs, with the proportion of GluR2 relative to the other mRNAs varying from 1:10 to 10:1. Then the Woodhull affinity parameter for internal polyamine block, the barium-to-monovalent-cation permeability ratio, and the degree of block of kainate-induced currents by 1 mM external spermine were measured in each cell 2–4 d after injection.

If the simple presence or absence of GluR2 in a receptor determined all aspects of AMPA receptor permeation and the

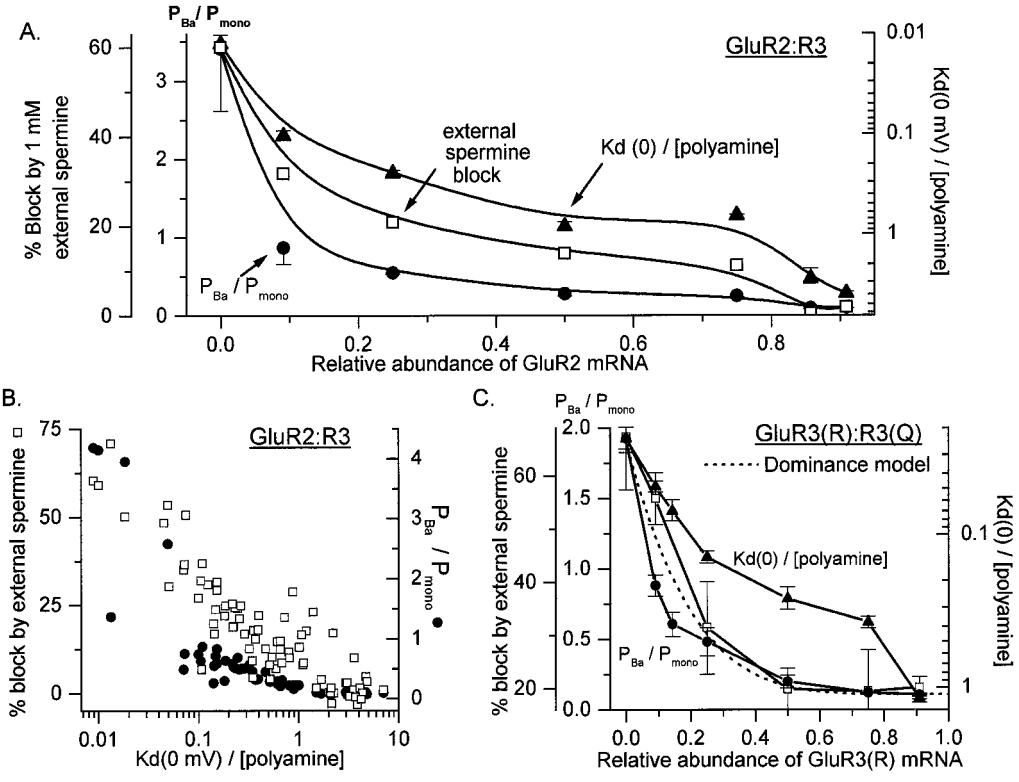

Figure 2. Different sensitivity of three permeation characteristics of AMPA receptors to the relative abundance of GluR2. *A*, Oocytes isolated from a single frog were microinjected with GluR2 and GluR3 mRNAs at different molar ratios of GluR2 and GluR3. After the oocytes were cultured for 2–3 d, the following measurements were made from each cell: $K_D(0)$/[polyamine] as fit by the Woodhull equations, $P_{Ba}/P_{monovalent}$ calculated from reversal potential measurements in high Na^+ and high Ba^{2+} medium, and the percentage block of kainate current at −70 mV elicited by 1 mM spermine. Data are expressed as a function of the GluR2 relative abundance, and the three measurements are scaled to permit comparisons. Each *point* represents the mean and SEM from four to six oocytes. *B*, Relation among the degree of block of kainate-evoked current by external spermine at −70 mV, the barium-to-monovalent permeability ratio, and the internal polyamine blocker affinity, as determined by the Woodhull model in oocytes injected with mixtures of GluR2 and 3 mRNAs. The ratio of GluR2 to GluR3 mRNAs was varied from 1:10 to 10:1 to produce receptors with a wide range of internal blocker affinity (n = 77 oocytes). *C*, Mixtures of GluR3(R612) and GluR3(Q612) were coinjected and a similar analysis performed as in *A* (n = 64 oocytes total). The *dotted line*, which represents the expected binomial abundance of receptors assembled with no GluR3(R) subunits, follows the equation $f(x_o) = \min + (\max - \min) \cdot (1 - x)^5$, where $f(x_o)$ is the fraction of receptors without GluR3(R) subunits, as a function of x = relative abundance of GluR3(R) protein in a functional receptor. Max and min represent the maximum and minimum GluR3(R)-dependent effect and were the only free variables.

effect of increasing GluR2 abundance was only to increase the proportion of receptors that assembled with a given number of GluR2 subunits (i.e., the fixed stoichiometry model), then all GluR2-dependent effects should be equally sensitive to the GluR2 expression level. The reasoning is similar to that described above for analyzing the shape of *I–V* curves (Fig. 1*A*). The fixed stoichiometry model requires that each macroscopic response be summed over a population of individual receptors, each of which can assume only one of two states, depending on the presence or absence of GluR2. If subunit stoichiometry is variable, on the other hand, the three phenotypic measures will show the same sensitivity to GluR2 abundance only if their molecular mechanisms are identical.

In violation of the prediction of the fixed stoichiometry model, the three phenotypic measures showed clearly different sensitivities to the relative abundance of GluR2 (Fig. 2*A*). To facilitate comparisons, each of the three measurements was scaled from its maximum value in the absence of GluR2 to its minimum value in the presence of saturating GluR2. In this experiment fourfold more GluR2 was required to reduce the log of internal blocker affinity by 50% than to reduce $P_{Ba}/P_{monovalent}$ by 50%, and the sensitivity of external spermine block to GluR2 was intermediate. This observed difference in GluR2 sensitivity for the three phenotypic features, measured in the same cells, is incompatible with a fixed number of GluR2 subunits in a receptor. Rather, this result indicates that the number of GluR2 subunits in AMPA receptors assembled in oocytes is variable. This result also confirms previous conclusions that the molecular determinants of rectification and divalent ion permeability are not identical (Burnashev et al., 1992; Dingledine et al., 1992). As a consequence of differential sensitivity to GluR2 abundance, both $P_{Ba}/P_{monovalent}$ and external spermine block were steep functions of internal blocker affinity when results from all injection ratios were plotted together (Fig. 2*B*). Meucci et al. (1996) also concluded that differences in calcium flux and block by argiotoxin-636 (ATX-636) in cortical glia might be explained by a variable number of GluR2 subunits in AMPA receptors, but their data could not rule out a fixed stoichiometry model.

$P_{Ba}/P_{monovalent}$ was a steeper function of GluR2 than Geiger et al. (1995) found in a population of interneurons (Fig. 2*A*), suggesting that under our conditions GluR2 translation and/or as-

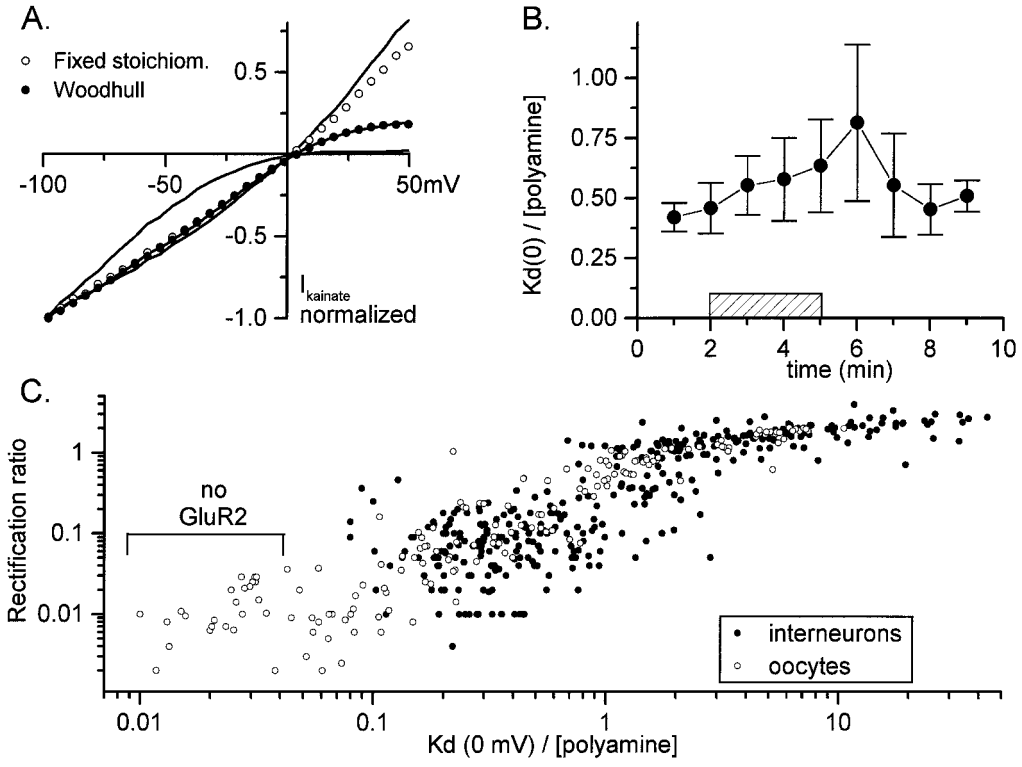

Figure 3. Variety and stability of internal blocker affinity in hippocampal interneurons. *A*, *I–V* curves from two different interneurons, selected to show the extremes of inward and outward rectification, and an interneuron showing intermediate rectification. The fixed stoichiometry model (*open circles*) consisting of the weighted average of the two extreme *I–V* curves (80% outward + 20% inwardly rectifying *I–V* curves) could fit the inward but not outward limb of the intermediate *I–V* curve. The Woodhull model [*filled circles*; $K_D(0)/[\text{polyamine}] = 1.48$, $z(1 - \delta) = 1.11$] fit well over both inward and outward limbs of the curve. *B*, Stability of measured internal blocker affinity during the first 10 min after achieving whole-cell voltage clamp. Kainate currents were evoked every minute in neurons selected for initially high internal blocker affinity. Each *point* represents the mean and SEM from three to nine cells. The *hatched bar* illustrates the time window for sampling neurons for the single-cell RT-PCR analysis. *C*, Direct comparison of rectification properties of AMPA receptors expressed by interneurons and oocytes. Each *point* represents measurements from a different interneuron ($n = 354$) or oocyte ($n = 170$). Plots of data from the two cell types are superimposable except for the extreme GluR2-lacking recombinant receptors, which appear to be absent from the interneuron population.

sembly is more efficient than that of GluR3. Relative translation efficiency is influenced by the structure of the mRNAs (5′ and 3′ UTRs, etc.). The design of this experiment does not depend on any particular relation between mRNA abundance and the abundance of assembled GluR2 in functional receptors, because all three measurements were made in the same oocyte. However, to circumvent possible problems with differential assembly of subunits, we coinjected mixtures of GluR3(Q612) and GluR3(R612) and obtained the three measures as above. As before, rectification was much less sensitive to GluR3(R) abundance than the other two features (Fig. 2*C*). The dashed curve in Figure 2*C* reflects the binomial abundance of pentameric AMPA receptors containing no GluR3(R) subunits. This "dominance" model for the effectiveness of arginine-containing subunits (Geiger et al., 1995) provides a reasonable fit to the curves of P_{Ba}/P_{mono} and external spermine block, consistent with a single GluR3(R) subunit being sufficient to completely convert these features of the AMPA receptor. However, it is clear that additional GluR3(R) subunits are required to abolish rectification, which has a gradual relation to GluR3(R) abundance.

A substantial difference in response of these three measures also was observed when GluR2(R586) was coinjected with GluR2(Q586) (data not shown). Thus, the different sensitivity of internal blocker affinity and divalent cation permeability to GluR2 level is controlled solely by the number of arginines in the Q/R site, regardless of the subunit source of these arginines. These data indicate that more arginine-bearing subunits are required in a receptor to linearize the *I–V* relation than to abolish divalent permeability or external polyamine block.

Internal polyamine block and calcium permeability in interneurons

To determine whether native AMPA receptors in neurons can exhibit the same variable subunit stoichiometry as occurs with recombinant receptors assembled by oocytes, we studied the interneuron population of CA3 stratum radiatum, which had been classified previously as type 1 (linear *I–V* curve) or type 2 (inwardly rectifying *I–V*) cells (McBain and Dingledine, 1993). Acutely isolated interneurons were prepared to achieve better voltage control and cleaner access to cellular RNA than is possible in slices. The *I–V* relation of kainate-activated currents determined from a total of 581 acutely isolated neurons in the whole-cell patch configuration showed a wide range of rectification ratios. Because the stoichiometry of subunit assembly might be controlled more stringently in neurons than in oocytes, we first considered whether a fixed stoichiometry model for AMPA receptors could explain this observation. However, similar to the findings with recombinant receptors in oocytes (Fig. 1*A*), the *I–V*

curves of interneurons with intermediate degrees of rectification were not well described by the weighted average of *I–V* relations selected from the extremes of the interneuron population (Fig. 3*A*, *open circles*).

Then the *I–V* curves of ~400 neurons were fit by the Woodhull model, which did provide good fits for cells with intermediate degrees of rectification (e.g., Figs. 3*A*, 5*B*). The Woodhull affinity parameter was stable over at least the first 5 min of recording in the whole-cell mode (Fig. 3*B*), suggesting that washout of internal polyamines was negligible during this period. In neurons harvested for RT-PCR (see below), the kainate *I–V* relation was measured 2–5 min after achieving the whole-cell configuration (Fig. 3*B*, *hatched box*) and therefore accurately reflected the rectification properties of native AMPA receptors in intact neurons.

The rectification ratio and internal blocker affinity varied over approximately three orders of magnitude (Fig. 3*C*), suggestive of very heterogeneous AMPA receptor expression in this interneuron population. The histogram of $K_D(0)$/[polyamine] was bimodal, with an inwardly rectifying (corresponding to the previously defined type 2) population having a mode of 0.18–0.22, a second broad peak representing type 1 neurons at a mode of 1.5–6, and a tail extending beyond 30. For comparison with previous studies, neurons with $K_D(0)$/[polyamine] < 0.5 have rectification ratios <0.3 and correspond to type 2 cells, whereas those with $K_D(0)$/[polyamine] > 3 are type 1 cells with rectification ratios >1 (Fig. 3*C*). The "intermediate" or "type 3" neurons previously identified as those with rectification ratios lying between the two extremes (Iino et al., 1994; Lerma et al., 1994) are probably neurons on the shoulders of the two broad populations identified here.

Data obtained from both oocytes and interneurons are nearly completely overlapping (Fig. 3*C*). This suggests that the Woodhull model is as appropriate for oocytes as it is for interneurons. Note that the interneuron population apparently did not contain cells with the highest affinity internal block, which is characteristic of recombinant AMPA receptors lacking GluR2 (Fig. 3*C*).

Similar to findings reported for other hippocampal interneurons (Iino et al., 1990, 1994; Lerma et al., 1994), AMPA receptors expressed by neurons with strong internal channel block exhibited high calcium permeability, as evidenced by a positive shift in reversal potential of kainate-induced currents on switching from high Na^+ to high Ca^{2+} solution (Fig. 4*A, left panel*). In contrast, AMPA receptor channels of neurons with weak internal polyamine block were much less permeable to calcium, indicated by a large negative shift in kainate reversal potential (up to −60 mV) on switching from high Na^+ to high Ca^{2+} medium (Fig. 4*A, right panel*). P_{Ca}/P_{Na} fell sharply as a function of internal blocker affinity in a sample of 39 neurons in which both parameters had been measured (Fig. 4*C*, *solid circles*), although appreciable calcium permeability ($P_{Ca}/P_{Na} > 0.3$) was observed in some cells with low internal blocker affinity. P_{Ca}/P_{Na} ranged from ~5 to 0.01 in this interneuron population, corresponding to a fractional calcium influx (at −70 mV and 1.5 mM $[Ca]_{out}$) of 0.01–3.6% (Burnashev et al., 1995).

External polyamine block

Polyamine spider toxins selectively block GluR2-lacking recombinant AMPA receptors (Blaschke et al., 1993; Brackley et al., 1993; Herlitze et al., 1993; Washburn and Dingledine, 1996). Accordingly, 1 μM ATX-636 produced a voltage-dependent block of the inwardly rectifying kainate current in cells with strong internal blocker affinity (Fig. 4*B, left panel*), whereas ATX-636 had little or no effect on cells with weak internal block (Fig. 4*B, right panel*).

Selective block of inwardly rectifying AMPA receptors was observed with other polyamine spider toxins, including Agel-489, Joro spider toxin, philanthotoxin-433, and argiotoxin-659, and with spermine itself. In 48 interneurons tested with concentrations of these polyamines shown to be near-maximally effective on recombinant GluR3 receptors (Washburn and Dingledine, 1996), the degree of channel block by external polyamines declined sharply as internal blocker affinity decreased (Fig. 4*C*). This result, and that of Figure 2*A*, suggests that some native and recombinant AMPA receptors with substantial inward rectification can exhibit minimal divalent ion permeability and minimal sensitivity to channel block by external polyamines. The degree of block by 1 mM spermine at −70 mV shows a similar relation to rectification properties of AMPA receptors expressed in oocytes and interneurons (compare □ in Figs. 2*B* and 4*C*).

In 18 interneurons we directly compared the calculated affinities of internal polyamine and external ATX-636 for their respective blocking sites in the channel. As expected, the affinities for external and internal block covaried (Fig. 4*D*), but interestingly the affinity for external argiotoxin block was approximately four times as sensitive to the underlying controlling variable (presumably GluR2 abundance) than was the internal blocker affinity, as indicated by the slope of the dashed line in Figure 4*D*. This is consistent with the observed difference in sensitivity to GluR2 abundance for these two parameters studied in recombinant receptors expressed in oocytes (Fig. 2*B*).

Combined genetic and physiological analyses

A multiplex RT-PCR assay was designed to detect which of the four AMPA receptor mRNAs are expressed in individual interneurons. A two-stage nested PCR was used, in which pan primers that anneal to homologous regions of the four AMPA receptor sequences were used in a first round of PCR; this PCR product was purified, and aliquots were amplified separately with four individual primer pairs specific to GluR1, 2, 3, and 4. Preliminary experiments demonstrated a number of points. First, mixtures of 100 fg of each of the four cRNAs could be reverse-transcribed reliably and amplified, whereas mixtures of nominally 1 fg each (adsorption to pipette and tube walls probably reduced the actual amount of carrier-free cRNA) were amplified inconsistently. Second, each of the nested second-round PCR primer pairs selectively amplified only the expected GluR sequence under the conditions used. Third, two-stage RT-PCR of 2 pg of whole rat brain RNA produced clear ethidium-stained DNA bands in an agarose gel; each of the four bands had the expected sizes and restriction digest patterns (Lambolez et al., 1992).

For the cells studied here we used $K_D(0)$/[polyamine] as the electrophysiological index that was correlated with AMPA receptor subunit expression, because harvest of the cell then could be accomplished within 5 min of breaking through to the whole-cell recording mode. In 282 isolated neurons the entire cell was harvested under visual control after electrophysiological characterization of the response to kainate. For 85 cells, PCR bands indicative of one or more AMPA receptor subunits were recovered, but control amplification of bathing medium aspirated from the recording chamber produced no PCR bands. *I–V* relations were adequately fit by the Woodhull

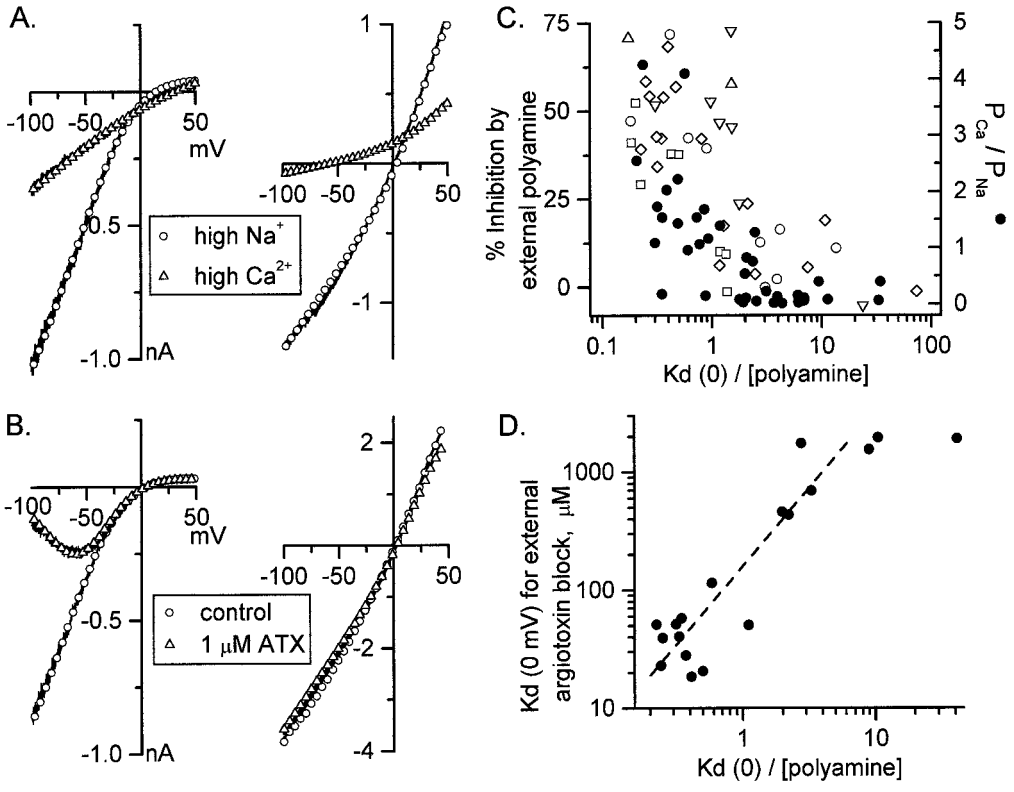

Figure 4. Differential calcium permeability and sensitivity of kainate currents to block by polyamine toxins in isolated interneurons. *A*, The kainate reversal potential shifted from +13.6 to +30.4 mV in an interneuron with inwardly rectifying kainate *I–V* relation when the bathing solution was changed from high Na^+ to high Ca^{2+} solution (*left panel*). The Woodhull fits to the two curves are superimposed [*open circles* for the high Na^+ curve; $K_D(0)/[\text{polyamine}] = 0.29$, $z(1-\delta) = 0.98$]. In contrast, an interneuron with weak blocker affinity [*right panel*; $K_D(0)/[\text{polyamine}] = 16.2$ with $z(1-\delta) = 1.25$] showed a large negative shift in kainate reversal potential (from +3.1 to −57 mV) when the bathing medium was changed from high Na^+ to high Ca^{2+}. *B*, Kainate-evoked current in an interneuron with strong internal block [*left panel*; $K_D(0)/[\text{polyamine}] = 0.20$, $z(1-\delta) = 0.92$] is inhibited in a voltage-dependent manner by 1 μM ATX-636. The *open circles* represent the Woodhull model fits in the absence of argiotoxin, and the *open triangles* represent Woodhull fits in the presence of the external polyamine toxin. Kainate currents in an interneuron with weak internal blocker affinity [*right panel*; $K_D(0)/[\text{polyamine}] = 12.5$, $z(1-\delta) = 0.45$] are resistant to argiotoxin block. *C*, The calcium-to-sodium permeability ratio decreased sharply as a function of internal blocker affinity in a sample of 39 interneurons (*filled circles*). The *open symbols* show a summary of data from 48 interneurons, illustrating the block of kainate-evoked currents measured at −70 mV by five polyamine spider toxins and spermine. △, 3 μM philanthotoxin-433; ○, 3 μM Joro spider toxin; □, 1 mM spermine; ▽, 3 μM Agel-489 toxin from the funnel web spider, *Agelinopsis aperta*; ◇, 1 μM ATX-636. *D*, Correlation between measured affinities for internal and external channel block in interneurons. In each cell ($n = 18$) the kainate *I–V* curve was fit with the Woodhull equations to derive the affinity for internal block; then 1 μM ATX-636 was added to the external perfusing solution, and the kainate *I–V* curve was obtained again. The affinity of external argiotoxin for its channel-blocking site was determined by fits of the *I–V* curve as in *B* and plotted against the internal blocker affinity of the same neuron. The slope of a line fit to the initial rising phase ($K_D(0)/[\text{polyamine}]$ between 0.18 and 3.1 μM) is 4.2.

equation for internal block in 82 of these cells. Whereas the molecular analysis of AMPA receptor mRNAs in the majority of cells yielded results consistent with properties of recombinant heteromeric AMPA receptors, it was notable that many interneurons with strong inward rectification expressed GluR2 mRNA (e.g., Fig. 5*C*).

We considered and then rejected two explanations for the presence of GluR2 mRNA in neurons expressing AMPA receptors with strong inward rectification. First, the likelihood that inward rectification in type 2 interneurons is attributable to the expression of unedited GluR2 mRNA (Sommer et al., 1991) is low, given that the unedited form of GluR2 is present in only 0.01% of total GluR2 mRNA in early postnatal stages (Burnashev et al., 1992). Indeed, *Bbv*I restriction digests of GluR2 RT-PCR bands, which produced a 106 bp band diagnostic of unedited GluR2(Q), verified that the Q/R site was edited virtually completely in the cell shown in Figure 5*C* and in one other examined (data not shown). The *Bbv*I digestion products of both cells ran identically on an agarose gel to those of authentic GluR2(R) RT-PCR bands that had been digested with *Bbv*I. Second, it is also unlikely that some of the GluR2-positive type 2 cells expressed functional kainate receptors exclusively rather than AMPA receptors (Ruano et al., 1995), because kainate-evoked currents could be large and were not rapidly desensitizing in these cells (cf. Egebjerg et al., 1991; Dingledine et al., 1992). Moreover, 100 μM cyclothiazide potentiated kainate-evoked currents in both type 1 and 2 interneurons by 2.2 ± 0.2-fold ($n = 8$ interneurons; data not shown), as expected if kainate currents are mediated mainly by AMPA receptors in these neurons (Partin et al., 1993). This is somewhat smaller than the 4.3-fold potentiation reported after preincubation of cultured hippocampal neurons in cyclothiazide (Partin et al., 1993, 1996), which likely is attributable to differences in flip/flop expression as well as to differences in application procedures in the two studies [Partin et al. (1993) reported a superimposed inhibitory effect of co-perfused cyclothiazide]. Although we cannot rule out the possibility that the

acute dissociation process induced the synthesis of GluR2 mRNA that had not been incorporated into functional receptors in type 2 cells by the time of recording, a more parsimonious explanation for the presence of GluR2 mRNA in type 2 cells lies with our observation that rectification itself is not very sensitive to low GluR2 mRNA abundance (Figs. 1, 2).

Only approximately one-half (13 of 23) of neurons with highly inwardly rectifying kainate *I–V* relationships ($K_D(0) < 30$ μM) lacked detectable GluR2 mRNA. An example of such cells is shown in Figure 5*B*. Conversely, Figure 5*A* shows an interneuron with weak internal blocker affinity that exhibited large outwardly rectifying kainate currents and expressed all four AMPA receptor mRNAs. The results from all 82 neurons in which the combined genetic and physiological analyses were performed are summarized in Figure 5*D*. Because PCR amplification is highly nonlinear, and in controlled experiments the intensity of the ethidium-stained PCR bands did not correlate well with the amount of input cRNA in the 1–100 fg range, we designated neurons only as expressing or not expressing GluR2. The mean $K_D(0)$/[polyamine] for internal block in GluR2-lacking interneurons (2.61 ± 0.6, $n = 38$) was significantly lower than that for GluR2-expressing neurons (5.34 ± 1.35, $n = 44$; $p < 0.05$). However, 10 of 23 neurons with very pronounced inward rectification ($K_D(0)$/[polyamine] < 0.5) expressed the GluR2 subunit (Fig. 5*C*).

The expression pattern of the other AMPA receptor subunits was not obviously linked to GluR2 expression in neurons with inwardly rectifying AMPA receptors. Thus, for 13 type 2 cells that lacked GluR2, 5 expressed GluR1, 12 expressed GluR3, and 7 expressed GluR4 mRNA. By comparison, for the 10 type 2 cells that did express GluR2, 2 also expressed GluR1, 9 expressed GluR3, and 7 expressed GluR4. These data indicate that acutely isolated hippocampal interneurons with inwardly rectifying AMPA receptors appear to express virtually any combination of AMPA receptor subunit mRNAs. In particular, inward rectification is not incompatible with the presence of GluR2 mRNA in this population of hippocampal interneurons. This is consistent with our findings with recombinant receptors (Figs. 1, 2) but contrasts with Bochet et al. (1994), who reported that type 2 hippocampal neurons in culture never express GluR2 or GluR3 mRNAs, as judged by RT-PCR. The wide distribution of internal blocker affinities observed here is consistent with the finding of a range of GluR2 levels in different neuron types (Geiger et al., 1995), the recent finding that most hippocampal interneurons exhibit some degree of GluR2 immunoreactivity (Vissavajjhala et al., 1996), and our finding that internal blocker affinity is not very sensitive to the relative abundance of GluR2 in recombinant receptors (Figs. 1–3).

As expected, most (17 of 26) neurons with weak internal blocker affinity ($K_D(0)$/[polyamine] > 3) expressed the GluR2 subunit. Of the 17 GluR2-expressing type 1 neurons, 10 expressed GluR1, 15 expressed GluR3, and 10 expressed GluR4. Little can be concluded from the nine type 1 neurons that apparently lacked GluR2, because the apparent lack of GluR2 mRNA in type 1 cells may reflect the inability of our assay to detect mRNAs present in low copy number (see Materials and Methods).

DISCUSSION

These experiments were designed to answer two questions. First, is AMPA receptor subunit stoichiometry fixed or variable with respect to the GluR2 subunit? Second, do recombinant AMPA receptors expressed in *Xenopus* oocytes resemble those expressed by hippocampal interneurons? The three most significant findings of this study include the following: first, the extreme variability of rectification properties in both native and recombinant AMPA receptors is incompatible with a fixed stoichiometry model of subunit stoichiometry but can be described by the Woodhull channel block model only if internal blocker affinity is variable. Second, divalent ion permeability and channel block by externally applied polyamines in recombinant AMPA receptors are more sensitive to GluR2 mRNA abundance than is rectification. As predicted by this result, many type 2 interneurons exhibiting inwardly rectifying native AMPA receptors express detectable levels of GluR2 mRNA. Finally, the relationships among divalent ion permeability, the affinity for block by external polyamines, and internal blocker affinity are quantitatively similar in both native and recombinant AMPA receptors. These findings have a number of implications.

The difference in sensitivity of the three phenotypic features of AMPA receptor channels to GluR2 expression (Fig. 2*A*) suggests that more GluR2 subunits within an individual receptor are required to abolish inward rectification than are needed to maximally disrupt calcium influx. This conclusion is strengthened by the inability to fit simultaneously both the inward and outward limbs of *I–V* curves by weighted averages of *I–V* relations with extreme degrees of rectification (Figs. 1*A*, 3*A*) and by the need for *variable* internal blocker affinity to fit *I–V* relations to the Woodhull equation (Figs. 1*A,B,D*, 3*A*). None of these three findings is compatible with the alternative concept that cells simply express a mosaic of two populations of AMPA receptors that either have or lack GluR2 in a fixed stoichiometry. We cannot, however, rule out that preferred stoichiometries may exist, nor can the exact subunit stoichiometry be deduced from our data. In contrast to AMPA receptors, electrophysiological and biochemical data suggest that neuronal nicotinic, $GABA_A$, and glycine receptors all form subunit assemblies with fixed stoichiometries (Cooper et al., 1991; Kuhse et al., 1993; Kellenberger et al., 1997; Tretter et al., 1997), a concept that has been firmly established for muscle nicotinic receptors (Gu et al., 1991). The limited distribution of single channel conductance states for NMDA receptors assembled from NR2A plus combinations of wild-type and mutant NR1a subunits led Béhé et al. (1995) to propose that all NMDA receptors have exactly two NR1 subunits. Their data are not incompatible with multiple subunit stoichiometries that are functionally silent, however, as pointed out by the authors. Thus, in addition to differences in transmembrane topology between glutamate receptors and the other ligand-gated ion channels (Hollmann et al., 1994; Wo and Oswald, 1994; Bennett and Dingledine, 1995), the logic of subunit assembly seems different, endowing AMPA receptors with a much greater diversity than previously suspected.

Functional consequences of variable AMPA receptor stoichiometry

Neurons seem to achieve versatility in AMPA receptor properties in part by varying the *proportion* of GluR2 expressed with other subunits. A graded spectrum of synaptic AMPA receptors, rather than mixtures of the two extreme types either containing or lacking GluR2 as previously surmised (Iino et al., 1994; Jonas et al., 1994; Lerma et al., 1994; Goldstein et al., 1995; Seifert and Steinhauser, 1995), should allow interneurons to fine-tune the properties of synaptic currents mediated by AMPA receptors. GluR2 has two opposing effects on the amplitude of AMPA receptor currents. First, GluR2 should cause a graded increase in

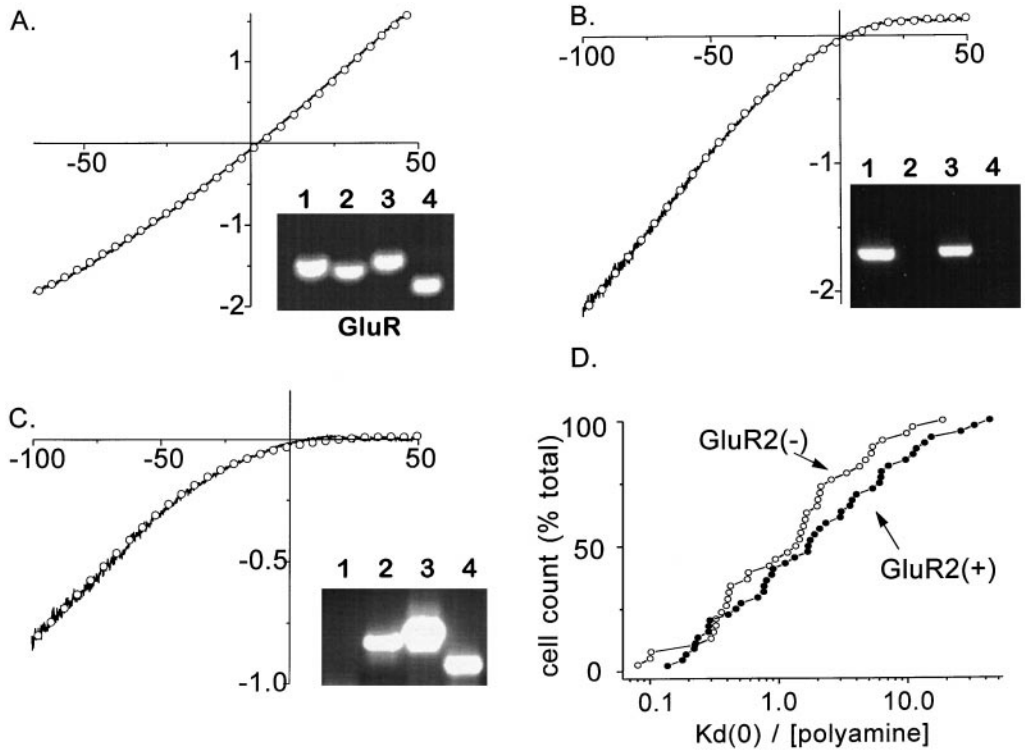

Figure 5. AMPA receptor subunit expression in physiologically characterized interneurons. *A*, An interneuron with outwardly rectifying kainate *I–V* relation that expressed all four AMPA receptor subunits by RT-PCR. The *inset* shows an agarose gel separation of RT-PCR products from this cell. The *open circles* are fits of the Woodhull equation [$K_D(0)/[\text{polyamine}] = 6.28$, $z(1 - \delta) = 1.01$]. *B*, Neuron with inwardly rectifying kainate current [$K_D(0)/[\text{polyamine}] = 0.33$, $z(1 - \delta) = 0.87$] that expressed GluR1 and GluR3 mRNAs, but not GluR2 or GluR4. *C*, *I–V* relation from an interneuron showing strong inward rectification [$K_D(0)/[\text{polyamine}] = 0.14$, $z(1 - \delta) = 0.92$]; this neuron expressed GluR2, GluR3, and GluR4 in sufficient amounts to be detected by RT-PCR. *D*, Cumulative distributions of the affinity of internal blocker for 38 interneurons lacking GluR2 mRNA and 44 interneurons that expressed GluR2.

synaptic currents at resting membrane potentials by up to ~50% because internal channel block is significant even at these negative membrane potentials (Bowie and Mayer, 1995) (see Figs. 1*A,B,D*, 3*A*). Second, GluR2 reduces single channel conductance of AMPA receptors by up to 70% without changing P_{open} (Swanson et al., 1997). The balance of these two opposing effects determines the overall effect of GluR2 abundance on EPSP amplitude. The findings that even small changes in EPSP amplitude can alter the ability of hippocampal pyramidal neurons to fire synchronously (Chamberlin et al., 1990; Traub and Dingledine, 1990) and that long-term potentiation is often characterized by a 50–100% increase in EPSP amplitude suggest that cell-to-cell differences in the level of GluR2 expression will be functionally significant beyond the simple control of calcium permeability. The functional consequences of variable GluR2 stoichiometry are likely to be particularly important in situations in which the GluR2:non-GluR2 ratio changes moderately (30–60%), such as after severe seizures (Pollard et al., 1993; Prince et al., 1995) or after chronic exposure to drugs of abuse (Fitzgerald et al., 1996). Our results suggest that in these conditions neurons with a normally high relative abundance of GluR2 (e.g., pyramidal cells and some interneurons) might respond to a fall in GluR2 abundance mainly with an increased rectification and change in EPSP amplitude, with relatively little increase in calcium permeability. In contrast, neurons with low relative GluR2 abundance (e.g., some interneurons) should respond mainly with increased calcium permeability through synaptic AMPA receptors.

Different structural determinants of divalent cation permeability and channel block by internal polyamines

The observed different sensitivities of calcium permeability and rectification to GluR2 abundance point to different molecular determinants, an idea also supported by mutations that dissociate rectification from divalent ion permeability and external polyamine block. Homomeric receptors composed of GluR3(Q612N) or GluR3(D616N) subunits exhibit high divalent cation permeability but possess outwardly or doubly rectifying kainate *I–V* relations (Burnashev et al., 1992; Dingledine et al., 1992). This finding suggests that elimination of the negatively charged carboxyl group on residue 616 markedly reduces the affinity of internal polyamines for their blocking sites. In contrast, spermine and external polyamine toxins still exert strong voltage-dependent block of channels composed of GluR3(D616N) or GluR3(Q612N) subunits (Herlitze et al., 1993; Washburn and Dingledine, 1996; M. Washburn and R. Dingledine, unpublished data), as expected if the internal and external blocking sites are not identical.

Why is rectification less sensitive to the relative abundance of GluR2 than is divalent permeability or block by external polyamines? Considering the role of the Q/R site in determining calcium permeability (Hume et al., 1991; Burnashev et al., 1992a), the role of the aspartates four residues downstream of Q/R in rectification (Dingledine et al., 1992; Washburn and Dingledine, 1996), and the finding that inward rectification is caused by internal

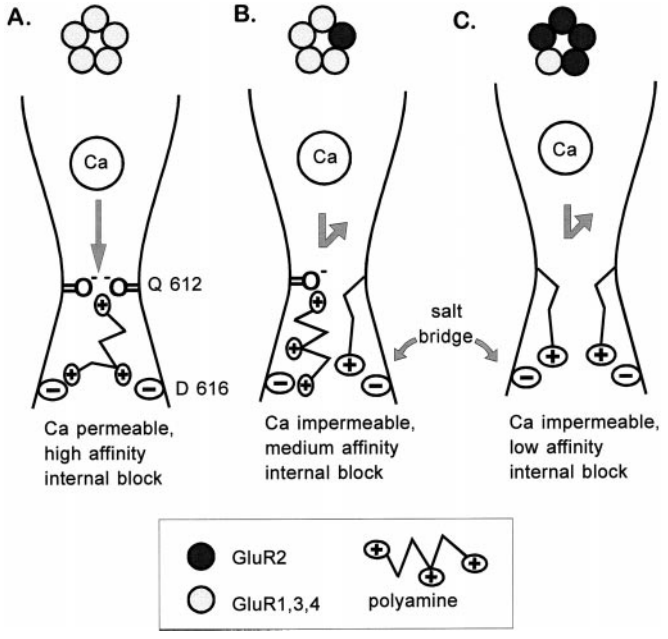

Figure 6. Model accounting for the differential dependence of calcium permeability and inward rectification on GluR2 abundance. In the model two amino acid residues determine the major permeation properties: a ring of aspartates that are found in all AMPA subunits and are predicted by transmembrane topology to be located near the cytoplasmic mouth of the channel (Hollmann et al., 1994; Wo and Oswald, 1994; Bennett and Dingledine, 1995) and the Q/R site located four residues upstream (Hume et al., 1991; Burnashev et al., 1992). The essence of the model is that the ring of carbonyl oxygens in GluR2-lacking AMPA receptors (*A*) contributes to or forms a binding site for permeating divalent cations. Internal polyamines also interact with this ring of polar residues and, by electrostatic interactions of the positively charged amine groups, with the carboxyl groups of the ionized aspartates at D616. Incorporation of a single positively charged arginine into the Q/R site (*B*) disrupts the ring of carbonyl groups, which is postulated to eliminate the divalent ion binding site. This arginine also neutralizes a negative charge at the internal channel mouth by formation of a salt bridge between its guanidinium group and the carboxyl group of the aspartate, which reduces the number of anionic binding sites for internal polyamines and thus decreases their affinity for the channel. As more arginines are incorporated into the Q/R site (*C*), the number of negative charges at the channel mouth, and hence polyamine affinity for the internal blocking site, is progressively reduced.

polyamine block (Bowie and Mayer, 1995; Donevan and Rogawski, 1995; Kamboj et al., 1995; Koh et al., 1995), we envision the following, mainly electrostatic, model (Fig. 6). In GluR2-lacking receptors, calcium and external polyamines are suggested to interact with a ring of carbonyl oxygens provided by glutamines residing at the Q/R site, calcium then permeating and the polyamines blocking the channel. In contrast, polyamines entering the channel from the cytoplasmic side cause inward rectification by binding to the Q/R site as well as to the ring of acidic carboxyl groups on the aspartates at residue 616 in GluR1, 3, or 4 (Fig. 6*A*). The additional contacts between the positively charged polyamines and these internal aspartates would be expected to stabilize binding at the Q/R site, contributing to the large observed difference in potency when spermine is applied from the cytoplasmic surface (IC_{50} at +40 mV = 0.3–1.0 μM; Bowie and Mayer, 1995; Kamboj et al., 1995) versus when applied extracellularly (IC_{50} at −70 mV = 160 μM; Washburn and Dingledine, 1996).

A single GluR2 subunit seems to be sufficient to maximally disrupt calcium permeability (Geiger et al., 1995). In the model a single arginine at the Q/R site may eliminate divalent cation permeability by disrupting the ring of carbonyl oxygens (Fig. 6*B*). By contrast, the shallower dependence of rectification on relative abundance of GluR2 (Fig. 2*A*) or GluR3(R612) (Fig. 2*C*) suggests that rectification is a graded function of the number of arginine-bearing subunits at the Q/R site (Fig. 6*B,C*). This could occur if positively charged arginine head groups at position 612 titrated away the negative charges at these aspartates and thereby removed internal binding sites that stabilize polyamines in the channel. Modelling of the M2 domain shows that the arginine side chain is long enough to form a salt bridge with the carboxyl groups four residues downstream if this region has α-helical or β-sheet or irregular secondary structure (R. Dingledine, unpublished data).

This model requires that internal polyamines block the channel by a multisite interaction. Two considerations support this idea. First, the mean value for $z(1 - \delta)$ measured in native AMPA receptors was 0.97 ± 0.014 (n = 361) and in oocytes 0.77 ± 0.018 (n = 113). With a mean valence of the blocking ion (z) of 3.8 (Traynelis et al., 1995), δ is 74–79% of the electrical distance from the extracellular side of the membrane. For an extended polyvalent blocker such as spermine, δ would represent a spatially smeared average of all binding sites within the channel. If the Q/R site lies near the middle of the membrane, as proposed for the NMDA receptor (Kuner et al., 1996), the observed value of δ is compatible with at least one additional contact site on the cytoplasmic side of the Q/R site contributing to block of AMPA channels by internal spermine. The second argument derives from a calculation of the binding energy of the blocker, $\Delta G = RT\ ln\ (K_{min}/K_{max})$, where K_{min}/K_{max} reflects a 1000-fold range of internal blocker affinity in recombinant and native AMPA receptors. Thus ΔG for internal block is ~4.0 kcal/mol, which is probably too large to reflect only a single point of interaction between the blocking ion and the channel. For example, if the dielectric constant at the surface of the channel is ~15 (Andersen and Koeppe, 1992; Honig and Nicholls, 1995), then each electrostatic interaction would contribute <2.3 kcal/mol (Andersen and Koeppe, 1992), and each polar interaction would contribute ~0.3 kcal/mol.

These conclusions do not depend on whether the AMPA receptor is a tetramer or pentamer, but for convenience a pentamer is illustrated. This model elaborates on previous attempts to understand the structural basis for rectification (Dingledine et al., 1992; Donevan and Rogawski, 1995). However, there is yet no direct evidence that D616 faces the open pore as required by the model. D616 is a conserved residue in all AMPA receptor subunits. Moreover, in GluR6(Q), which also is blocked by internal polyamines (Bowie and Mayer, 1995), a glutamate residue resides in the homologous position. In contrast, all known NMDA receptor subunits have a proline or glycine residue at the homologous position, which could account for their lack of inward rectification. Further tests of this model could involve NMDA receptors mutated at this site and quantitative measurements of the potency of spermine block from the inner membrane side in AMPA receptors bearing combinations of aspartates and asparagines at residue 616.

REFERENCES

Andersen OS, Koeppe RE (1992) Molecular determinants of channel function. Physiol Rev 72:S89–S149.

Béhé P, Stern P, Wyllie DJA, Nassar M, Schoepfer R, Colquhoun D

(1995) Determination of NMDA NR1 subunit copy number in recombinant NMDA receptors. Proc R Soc Lond [Biol] 262:205–213.

Bennett JA, Dingledine R (1995) Topology profile for a glutamate receptor: three transmembrane domains and a channel-lining reentrant membrane loop. Neuron 14:373–384.

Blaschke M, Keller BU, Rivosecchi R, Hollmann M, Heinemann S, Konnerth A (1993) A single amino acid determines the subunit-specific spider toxin block of α-amino-3-hydroxy-5-methylisoxazole-4-propionate/kainate receptor channels. Proc Natl Acad Sci USA 90:6528–6532.

Bochet P, Audinat E, Lambolez B, Crépel F, Rossier J, Iino M, Tsuzuki K, Ozawa S (1994) Subunit composition at the single-cell level explains functional properties of a glutamate-gated channel. Neuron 12:383–388.

Bowie D, Mayer ML (1995) Inward rectification of both AMPA and kainate subtype glutamate receptors generated by polyamine-mediated ion channel block. Neuron 15:453–462.

Brackley PT, Bell DR, Choi DK, Nakanishi K, Usherwood PN (1993) Selective antagonism of native and cloned kainate and NMDA receptors by polyamine-containing toxins. J Pharmacol Exp Ther 266:1573–1580.

Brusa R, Zimmerman F, Koh DS, Feldmeyer D, Glass P, Seeburg PH, Sprengel R (1995) Early-onset epilepsy and postnatal lethality associated with an editing-deficient GluR-B allele in mice. Science 270:1677–1680.

Burnashev N, Monyer H, Seeburg PH, Sakmann B (1992) Divalent ion permeability of AMPA receptor channels is dominated by the edited form of a single subunit. Neuron 8:189–198.

Burnashev N, Zhou Z, Neher E, Sakmann B (1995) Fractional calcium currents through recombinant GluR channels of the NMDA, AMPA, and kainate receptor subtypes. J Physiol (Lond) 485:403–418.

Burnashev N, Villarroel A, Sakmann B (1996) Dimensions and ion selectivity of recombinant AMPA and kainate receptor channels and their dependence on Q/R site residues. J Physiol (Lond) 496: 165–173.

Chamberlin NL, Traub RD, Dingledine R (1990) Role of EPSPs in initiation of spontaneous synchronized burst firing in rat hippocampal neurons bathed in high potassium. J Neurophysiol 64:1000–1008.

Cooper E, Couturier S, Ballivet M (1991) Pentameric structure and stoichiometry of a neuronal nicotinic acetylcholine receptor. Nature 350:235–238.

Dingledine R, Hume RI, Heinemann SF (1992) Structural determinants of barium permeation and rectification in non-NMDA glutamate receptor channels. J Neurosci 12:4080–4087.

Donevan SD, Rogawski MA (1995) Intracellular polyamines mediate inward rectification of Ca^{2+}-permeable α-amino-3-hydroxy-5-methyl-4-isoxazolepropionic acid receptors. Proc Natl Acad Sci USA 92:9298–9302.

Egebjerg J, Bettler B, Hermans-Borgmeyer I, Heinemann S (1991) Cloning of a cDNA for a glutamate receptor subunit activated by kainate but not AMPA. Nature 351:745–748.

Fitzgerald LW, Ortiz J, Hamedani AG, Nestler EJ (1996) Drugs of abuse and stress increase the expression of GluR1 and NMDAR1 glutamate receptor subunits in the rat ventral tegmental area: common adaptations among cross-desensitizing agents. J Neurosci 16:274–282.

Geiger JRP, Melcher T, Koh D-S, Sakmann B, Seeburg PH, Jonas P, Monyer H (1995) Relative abundance of subunit mRNAs determines gating and Ca^{2+} permeability of AMPA receptors in principal neurons and interneurons in rat CNS. Neuron 15:193–204.

Goldstein PA, Lee CJ, MacDermott AB (1995) Variable distributions of Ca^{2+}-permeable and Ca^{2+}-impermeable AMPA receptors on embryonic rat dorsal horn neurons. J Neurophysiol 73:2522–2534.

Gu Y, Forsayeth JR, Verrall S, Yu XM, Hall ZW (1991) Assembly of the mammalian muscle acetylcholine receptor in transfected COS cells. J Cell Biol 114:799–807.

Herlitze S, Raditsch M, Ruppersberg JP, Jahn W, Monyer H, Schoepfer R, Witzemann V (1993) Argiotoxin detects molecular differences in AMPA receptor channels. Neuron 10:1131–1140.

Hoch DB, Dingledine R (1986) GABAergic neurons in rat hippocampal culture. Brain Res 25:53–64.

Hollmann M, Hartley M, Heinemann S (1991) Ca^{2+} permeability of KA-AMPA-gated glutamate receptor channels depends on subunit composition. Science 252:851–853.

Hollmann M, Maron C, Heinemann S (1994) N-glycosylation site tagging suggests a three transmembrane domain topology for the glutamate receptor GluR1. Neuron 13:1331–1343.

Honig B, Nicholls A (1995) Classical electrostatics in biology and chemistry. Science 268:1144–1149.

Hume RI, Dingledine R, Heinemann S (1991) Identification of a site in glutamate receptor subunits that controls calcium permeability. Science 253:1028–1031.

Iino M, Ozawa S, Tsuzuki K (1990) Permeation of calcium through excitatory amino acid receptor channels in cultured rat hippocampal neurones. J Physiol (Lond) 424:151–165.

Iino M, Mochizuki S, Ozawa S (1994) Relationship between calcium permeability and rectification properties of AMPA receptors in cultured rat hippocampal neurons. Neurosci Lett 173:14–16.

Jia Z, Agopyan N, Miu P, Xiong Z, Henderson J, Gerlai R, Taverna FA, Velumian A, MacDonald J, Carlen P, Abramow-Newerly W, Roder J (1996) Enhanced LTP in mice deficient in the AMPA receptor GluR2. Neuron 17:945–956.

Jonas P, Racca C, Sakmann B, Seeburg PH, Monyer H (1994) Differences in Ca^{2+} permeability of AMPA-type glutamate receptor channels in neocortical neurons caused by differential GluR-B subunit expression. Neuron 12:1281–1289.

Kamboj SK, Swanson GT, Cull-Candy SG (1995) Intracellular spermine confers rectification on rat calcium-permeable AMPA and kainate receptors. J Physiol (Lond) 486:297–303.

Kellenberger S, Eckenstein S, Baur R, Malherbe P, Buhr A, Sigel E (1997) Subunit stoichiometry of oligomeric membrane proteins: $GABA_A$ receptors isolated by selective immunoprecipitation from the cell surface. Neuropharmacology 35:1403–1411.

Koh D-S, Burnashev N, Jonas P (1995) Block of native Ca^{2+}-permeable AMPA receptors in rat brain by intracellular polyamines generates double rectification. J Physiol (Lond) 486:305–312.

Kuhse J, Laube B, Magelei D, Betz H (1993) Assembly of the inhibitory glycine receptor: identification of amino acid motifs governing subunit stoichiometry. Neuron 11:1049–1056.

Kuner T, Wollmuth LP, Karlin A, Seeburg PH, Sakmann B (1996) Structure of the NMDA receptor channel M2 segment inferred from the accessibility of substituted cysteines. Neuron 17:343–352.

Lambolez B, Audinat E, Bochet P, Crépel F, Rossier J (1992) AMPA receptor subunits expressed by single Purkinje cells. Neuron 9:247–258.

Lerma J, Morales M, Ibarz JM, Somohano F (1994) Rectification properties and Ca^{2+} permeability of glutamate receptor channels in hippocampal cells. Eur J Neurosci 6:1080–1088.

Mackler SA, Eberwine JH (1993) Diversity of glutamate receptor subunit mRNA expression within live hippocampal CA1 neurons. Mol Pharmacol 44:308–315.

McBain CJ, Dingledine R (1993) Heterogeneity of synaptic glutamate receptors on CA3 stratum radiatum interneurones of rat hippocampus. J Physiol (Lond) 462:373–392.

Meucci O, Fatatis A, Holzwarth JA, Miller RJ (1996) Developmental regulation of the toxin sensitivity of Ca^{2+}-permeable AMPA receptors in cortical glia. J Neurosci 16:519–530.

Osborne HB, Mulner-Lorillon O, Marot J, Belle R (1989) Polyamine levels during *Xenopus laevis* oogenesis: a role in oocyte competence to meiotic resumption. Biochim Biophys Acta 158:520–526.

Partin KM, Patneau DK, Winters CA, Mayer ML, Buonanno A (1993) Selective modulation of desensitization at AMPA versus kainate receptors by cyclothiazide and concanavalin A. Neuron 11:1069–1082.

Partin KM, Fleck MW, Mayer ML (1996) AMPA receptor flip/flop mutants affecting deactivation, desensitization, and modulation by cyclothiazide, aniracetam, and thiocyanate. J Neurosci 16:6634–6647.

Pelligrini-Giampietro DE, Zukin RS, Bennett MVL, Cho S, Pulsinelli WA (1992a) Switch in glutamate receptor subunit gene expression in CA1 subfield of hippocampus following global ischemia in rats. Proc Natl Acad Sci USA 89:10499–10503.

Pelligrini-Giampietro DE, Bennett MV, Zukin RS (1992b) Are Ca^{2+}-permeable kainate/AMPA receptors more abundant in immature brain? Neurosci Lett 144:65–69.

Pollard H, Héron A, Moreau J, Ben-Ari Y, Khrestchatisky M (1993) Alterations of the GluR-B AMPA receptor subunit flip/flop expression in kainate-induced epilepsy and ischemia. Neuroscience 57:545–554.

Prince HK, Conn PJ, Blackstone CD, Huganir RL, Levey AI (1995) Downregulation of AMPA receptor subunit GluR2 in amygdaloid kindling. J Neurochem 64:462–465.

Ruano D, Lambolez B, Rossier J, Paternain AV, Lerma J (1995) Kainate receptor subunits expressed in single cultured hippocampal neurons: molecular and functional variants by RNA editing. Neuron 14:1009–1017.

Seifert G, Steinhauser C (1995) Glial cells in the mouse hippocampus express AMPA receptors with an intermediate Ca^{2+} sensitivity. Eur J Neurosci 7:1872–1881.

Sommer B, Kohler M, Sprengel R, Seeburg PH (1991) RNA editing in brain controls a determinant of ion flow in glutamate-gated channels. Cell 67:11–19.

Swanson GT, Kamboj SK, Cull-Candy SG (1997) Single-channel properties of recombinant AMPA receptors depend on RNA editing, splice variation, and subunit composition. J Neurosci 17:58–69.

Traub R, Dingledine R (1990) Simulation of spontaneous burst-firing in high potassium: role of spontaneous EPSPs in burst initiation. J Neurophysiol 64:1009–1018.

Traynelis SF, Hartley M, Heinemann SF (1995) Control of proton sensitivity of the NMDA receptor by RNA splicing and polyamines. Science 268:873–876.

Tretter V, Ehya N, Fuchs K, Sieghart W (1997) Stoichiometry and assembly of a recombinant $GABA_A$ receptor subtype. J Neurosci 17:2728–2737.

Vissavajjhala P, Janssen WGM, Hu Y, Gazzaley AH, Moran T, Hof PR, Morrison JH (1996) Synaptic distribution of the AMPA-GluR2 subunit and its colocalization with calcium-binding proteins in rat cerebral cortex: an immunohistochemical study using a GluR2-specific monoclonal antibody. Exp Neurol 142:296–312.

Washburn MS, Dingledine R (1996) Block of α-amino-3-hydroxy-5-methyl-4-isoxazolepropionic acid (AMPA) receptors by polyamines and polyamine toxins. J Pharmacol Exp Ther 278:669–678.

Wo ZG, Oswald RE (1994) Transmembrane topology of two kainate receptor subunits revealed by N-glycosylation. Proc Natl Acad Sci USA 91:7154–7158.